AFIT/GEO/EE/79-4

(6) PHASE RETRIEVAL USING AN
IMAGING SENSOR.

(9) Master's THESIS,

(14) AFIT/GEO/EE/79-4 (10) Charles V. /Scull
Capt   USAF

(11) Dec 79   (12)
                66

Approved for public release; distribution unlimited.

012225

PHASE RETRIEVAL USING AN

IMAGING SENSOR

THESIS

Presented to the Faculty of the School of Engineering

of the Air Force Institute of Technology

Air Training Command

in Partial Fulfillment of the

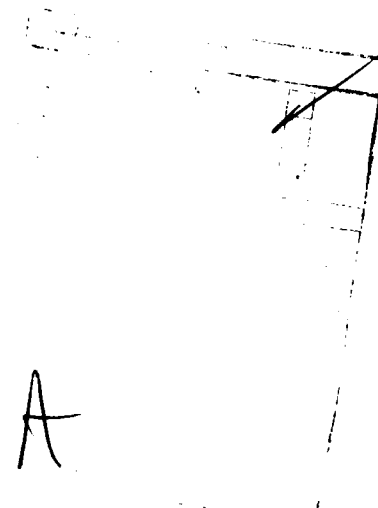Requirements for the Degree of

Master of Science

by

Charles V. Scull, B. S.

Capt   USAF

Graduate Electro-Optics

December 1979

Approved for public release; distribution unlimited

PREFACE

This thesis was sponsored by the Air Force Weapons Laboratory, Kirtland Air Force Base, New Mexico. It includes analytical and numerical methods to study the problem of retrieving spatial (relative) phase from intensity measurements in the focal plane of an imaging system. The author assumes the reader has a working knowledge of linear systems, Fourier transforms and Fourier optics.

I would like to thank Major Glenn Doughty and Professor Peter Maybeck for serving as readers contributing to this research. I am deeply grateful to my thesis advisor Captain Stanley Robinson for his guidance and assistance during this research study.

<div style="text-align: right">Charles V. Scull</div>

Contents

Contents

List of Figures

List of Tables

ABSTRACT

This research study is concerned with spatial (relative) phase reconstruction using an imaging sensor. Specifically, work was completed which investigates the retrieval of the spatial phase of the aperture wavefront from sampled intensity data in the focal plane of an imaging sensor, where phase is not explicitly present.

Techniques investigated are not interferometric methods, but are signal processing techniques that use the Fourier transform properties of a lens, analytics, and numerics to retrieve the spatial phase of the aperture field from intensity measurements in the focal plane of an imaging sensor. The techniques investigated include an analytic approach which is used to develop several numerical approaches, and the Gerchberg-Saxton Algorithm which is adapted to solve this specific phase retrieval problem. Finally, the results from simulations of these methods are compared yielding the Gerchberg-Saxton Algorithm as the most promising method to approximate the relative phase in the aperture plane.

PHASE RETRIEVAL USING AN
IMAGING SENSOR

I Introduction

The performance of state-of-the-art imaging sensors is limited by anomalies such as the turbulent atmosphere and aberations introduced by the optics of the sensor. As optical radiation propagates outward from its source the turbulence (random fluctuations in the refractive index) in the atmosphere distort the shape of the optical wavefront as well as cause intensity fluctuations across the optical wavefront. The random distortions in the shape of the optical wavefront are the primary contributors to the degradation of image quality in imaging systems (Refs 1 and 2).

In order to maximize image quality and resolving power of an imaging sensor, real-time active optical systems can be used to compensate for the distortions in the shape of the optical wavefront, adjusting the optical path length of the rays of each wavefront to be equal. Active optical systems consist of three main components; these are: a wavefront sensor (estimates the distortion in the optical wavefront), active optics (such as deformable mirrors) in the imaging sensor, and a feedback loop (Ref 2). A Wavefront sensor is an important component in closed-loop active optical systems. This research project is concerned

with using signal processing techniques to approximate the optical wavefront distortions incident on an imaging sensor.

Background

State-of-the-art imaging systems use interferometers to sense wavefront distortions, since detectors measure intensity of the electric field and can not directly measure the phase of a field. The basic configuration of an imaging system using an interferometer to sense wavefront distortions is shown in Figure 1. The limitations of these active optical systems are that they require two sensors, one for wavefront estimation and a second sensor for imaging, adding complexity to the system increasing the size, weight, and cost (acquisition and maintenance). The use of a beamsplitter (inherent in this class of imaging systems) makes the system more susceptible to noise (Refs 1 and 3).

Currently there is interest in developing a signal processing technique that can be used to retrieve the phase of the aperture field from intensity measurements in the focal plane of an imaging sensor, where phase is not explicitly present (Fig 2). There are two distinct advantages for using signal processing techniques instead of interferometric techniques for wavefront sensing in imaging sensors. The first advantage is that only one sensor is required for imaging, since intensity data in the focal plane can be measured with state-of-the-art detectors. The second

2
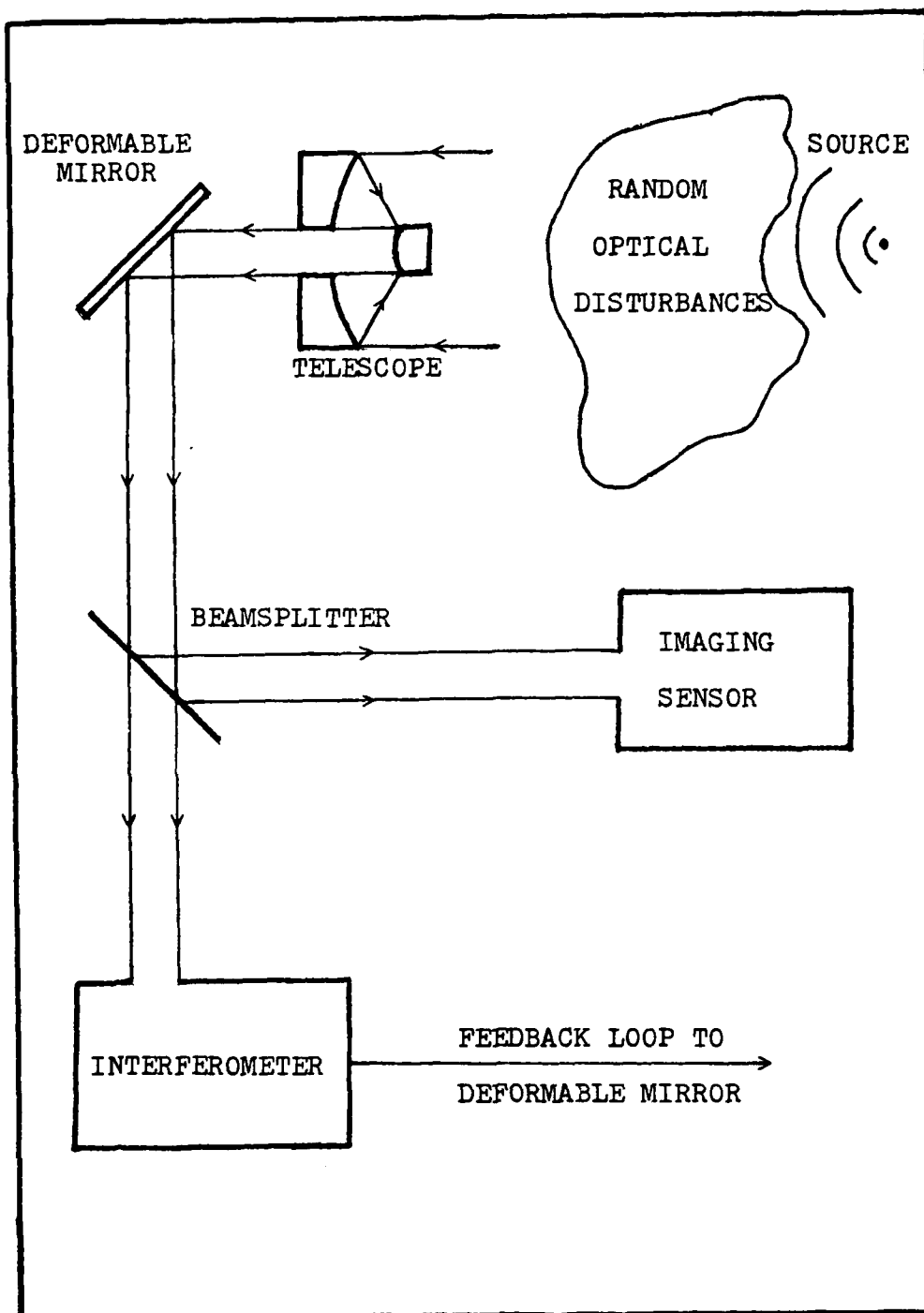
Figure 1. Basic configuration of an imaging system using an interferometer for wavefront sensing
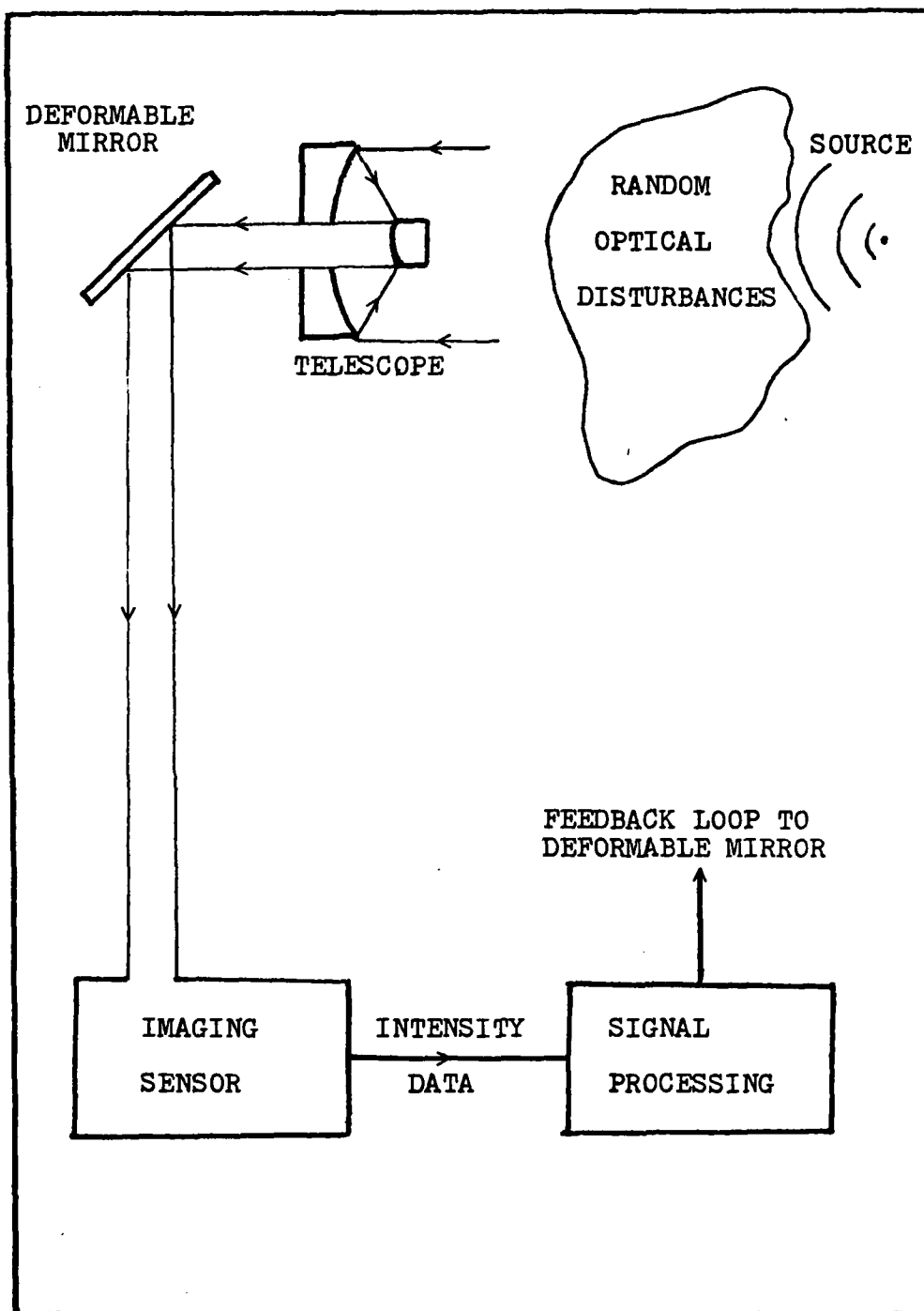
Figure 2. Basic configuration of an imaging system using signal processing of intensity data to retrieve the phase of the wavefront

advantage is that the signal processing technique does not require the use of a beamsplitter, and does not reduce image intensity which is especially important in systems where the intensity of the source can not be increased or can only be increased at the expense of the flexibility of a system (size, weight, and cost).

The problem of estimating the phase of an aperture field from intensity measurements in the focal plane is not a new one and is commonly referred to in the literature as the phase retrieval problem. This phase retrieval problem has many applications in other areas, such as: x-ray crystallography, particle scattering, optical communications, radar, and lens testing (Refs 2,4,5,6,7,8, and 9).

Problem Statement

The object of this thesis is to study techniques which can be used to retrieve the spatial (relative) phase of a complex (consisting of real and imaginary parts) wavefront incident on an imaging sensor, from intensity measurements in the focal plane of this sensor.

Approach

This research report is organized into five chapters: the Introduction, Formulation of the Problem, Phase Retrieval Techniques, Simulation Results and Analysis, and the Conclusion. The second chapter, Formulation of the Problem, develops the theory needed to retrieve the phase of the aperture field from intensity measurements in the focal plane of an imaging system. The third chapter, Phase

Retrieval Techniques, presents the two approaches used in this research study to infer the phase of the aperture field; these are: The Phase Analytic and Numeric Techniques, and the Gerchberg-Saxton Algorithm with and without feedback. The fourth chapter, Simulation Results and Analysis, defines the aperture wavefronts used in the simulation, the criterion used to rate the performance of the phase retrieval techniques simulated, and finally, presents the results and analysis of these phase retrieval techniques simulated as a function of one spatial variable. The fifth chapter, the Conclusion, is a summarization of the results of the research accomplished during this research study and recommends areas for further investigation.

II Formulation of the Problem

The purpose of this chapter is to develop the theory needed to retrieve the phase of the aperture field from intensity measurements in the focal plane of an imaging system. This research is concerned with the retrieval of the phase of a wavefront $(U_a(x_a,y_a))$, incident on the aperture of an imaging sensor, from intensity measurements $(I_m(x_f,y_f))$ in the focal plane of this sensor.

It is known from Fourier optics that the relationship between the focal plane $(U_f(x_f,y_f))$ and the aperture plane $(U_a(x_a,y_a))$ electric field (Fig 3) is given by

$$U_f(x_f,y_f) = \left(\frac{1}{j\lambda f}\right) exp\left(\frac{j2\pi f}{\lambda}\right) exp\left(\frac{\pi}{\lambda f}(x_f^2+y_f^2)\right)$$
$$\int\limits_{-\infty}^{\infty}\int\limits_{-\infty}^{\infty} U_a(x_a,y_a) exp\left(\frac{-j2\pi}{\lambda f}(x_f x_a + y_f y_a)\right) dx_a dy_a \quad (1)$$

The spatial Fourier transform is defined to be

$$\mathcal{F}_{xy}\left\{U_a(x_a,y_a)\right\} = \int\int U_a(x_a,y_a) exp\left(\frac{-j\pi}{\lambda f}(x_f x_a + y_f y_a)\right) dx_a dy_a \quad (2)$$

Substituting equation (2) into equation (1), the focal plane field is

$$U_f(x_f,y_f) = \left(\frac{1}{j\lambda f}\right) exp\left(\frac{j2\pi f}{\lambda}\right) exp\left(\frac{j\pi}{\lambda f}(x_f^2+y_f^2)\right) \mathcal{F}_{xy}\left\{U_a(x_a,y_a)\right\} \quad (3)$$
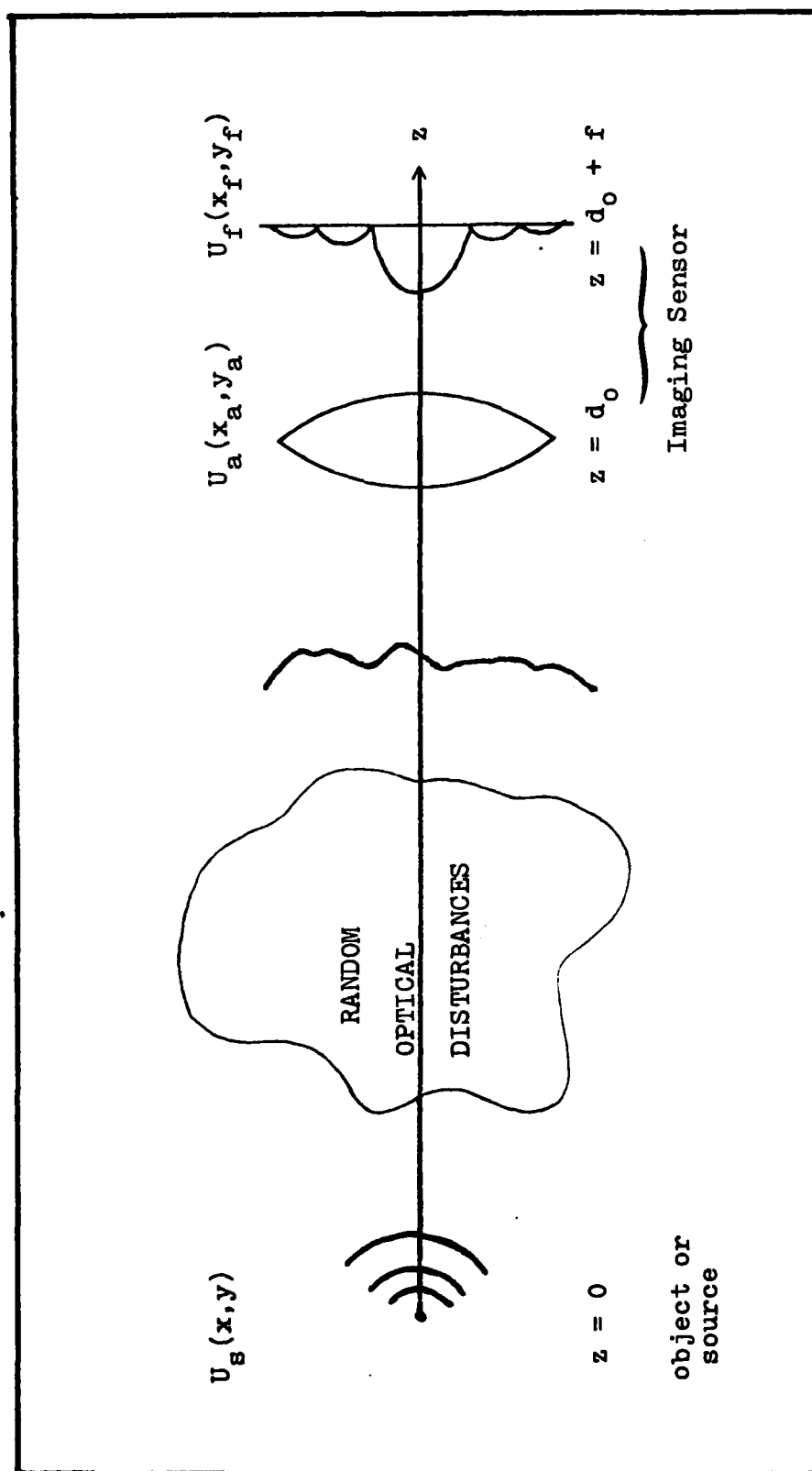
Figure 3. Simplified diagram of an imaging system

8

where

λ = the wavelength of the radiation

f = the focal length of the imaging sensor

f_x = spatial frequency in the focal plane (x direction)

f_y = spatial frequency in the focal plane (y direction)

Equation (3) is valid for monochromatic (single wavelength) radiation as well as quasi-monochromatic radiation. The conditions that must be met for radiation to be considered quasi-monochromatic are: the bandwidth (BW) of the radiation must be much less than the center frequency (v_o) of the radiation

$$\frac{BW}{V_o} << 1 \qquad (4)$$

and the reciprocal of the bandwidth must be greater than the length of the longest optical path (d) involved divided by the speed of light (c)

$$\frac{1}{BW} >> \frac{d}{c} \qquad (5)$$

(Ref 9).

We are concerned with an imaging sensor so intensity data in the focal plane ($I_m(x_f, y_f)$) is a measured quantity, and is the modulus of the electric field ($U_f(x_f, y_f)$)

9

$$I_m(x_f, y_f) = |U_f(x_f, y_f)| = U_f(x_f, y_f)\, U_f^{*}(x_f, y_f) \qquad (6)$$

where the asterisk (*) is used to denote the complex conjugate. The phase terms

$$\left(\frac{1}{\jmath}\right) exp\left(\frac{2\pi f}{\lambda}\right) exp\left(\jmath\frac{\pi}{\lambda f}\left(x_f^2 + y_f^2\right)\right) \qquad (7)$$

in equation (3) can be dropped for convenience since they are of no consequence in the measurement of the intensity in the focal plane. For simplicity the relationship between the focal plane and the aperture plane electric fields can be defined by the spatial Fourier transform relationship (except for a constant term), specifically

$$U_f(x_f, y_f) \cong \left(\frac{1}{\lambda f}\right) \int_{-\infty}^{\infty}\int_{-\infty}^{\infty} U_a(x_a, y_a)\, exp\left(\frac{-\jmath 2\pi}{\lambda f}\left(x_f x_a + y_f y_a\right)\right) dx_a\, dy_a \qquad (8)$$

$$\cong \left(\frac{1}{\lambda f}\right) \mathcal{F}_{xy}\left\{U_a(x_a, y_a)\right\} \qquad (9)$$

and

$$U_a(x_a, y_a) \cong \left(\frac{1}{\lambda f}\right) \int_{-\infty}^{\infty}\int_{-\infty}^{\infty} U_f(x_f, y_f)\, exp\left(\frac{\jmath 2\pi}{\lambda f}\left(x_f x_a + y_f y_a\right)\right) dx_f\, dy_f \qquad (10)$$

$$\cong \left(\frac{1}{\lambda f}\right) \mathcal{F}_{xy}^{-1}\left\{U_f(x_f, y_f)\right\} \qquad (11)$$

10

For a more thorough explanation of Fourier optics and the Fourier transform properties of a lens, refer to: "Introduction to Fourier Optics", by J.W. Goodman (Ref 9).

For mathematical simplicity it is assumed that the aperture wavefront is of unit magnitude and has a phase component $(w_a(x_a,y_a))$, where

$$U_a(x_a, y_a) = P\{x_a, y_a\} \exp(j\, w_a(x_a, y_a)) \tag{12}$$

The pupil function $(P(x_a,y_a))$ is

$$P\{x_a, y_a\} = \begin{cases} 1 & ; \; |x_a| < \frac{w_x}{2}, \; |y_a| < \frac{w_y}{2} \\ 0 & ; \; else \end{cases} \tag{13}$$

where

$\quad w_x$ = width of rectangular aperture in x direction

$\quad w_y$ = width of rectangular aperture in y direction

The phase component $(w_a(x_a,y_a))$ is the phase distortion in the aperture field that is to be retrieved in this research study. Now, substituting the aperture wavefront (equation (12)) into equation (8) an expression for the focal plane field is found

$$U_f(x_f, y_f) = \left(\frac{1}{\lambda f}\right) \int_{-\infty}^{\infty} \int_{-\infty}^{\infty} P(x_a, y_a) \exp\left(j W_a(x_a, y_a)\right)$$

$$\exp\left(\frac{-j2\pi}{\lambda f}\left(x_f x_a + y_f y_a\right)\right) dx_a dy_a \qquad (14)$$

Using equation (6) the intensity $(I_m(x_f, y_f))$ in the focal plane is found

$$I_m(x_f, y_f) = \int\int\int\int P_a(x_a, y_a) P_a(x_a', y_a') \exp\left(+j W_a(x_a, y_a) - W_a(x_a', y_a')\right)$$

$$\exp\left(-\frac{j2\pi}{\lambda f}\left(x_f(x_a - x_a') + y_f(y_a - y_a')\right)\right) dx_a dy_a dx_a' dy_a' \quad (15)$$

Equation (15) illustrates that even though there is no explicit phase information in the intensity measurement in the focal plane of an imaging sensor this intensity distribution is non-linearly related to the phase of the aperture field.

The development of the theory needed to investigate the retrieval of the phase of the aperture field from intensity measurements in the focal plane of an imaging system is now complete. The ideas and theory developed in this chapter are used in the phase retrieval techniques investigated in this thesis.

12

III Phase Retrieval Techniques

The purpose of this chapter is to present the phase
retrieval techniques investigated in this research project.
The chapter is divided into two sections. The first section
develops the Phase Analytic and Numeric Techniques. These
techniques represent the aperture plane wavefront in a
finite Fourier series and the approximates the Fourier
series coefficients as a method to reconstruct the aperture
field. The second section develops the Gerchberg-Saxton
Algorithm and a modified input-output approach. These
Gerchberg-Saxton Algorithm techniques directly retrieve
the aperture phase, i.e. they do not compute the Fourier
series coefficients.

Phase Analytic and Numeric Techniques

Analytic Approach. The first approach is directed
at developing an analytical solution to the phase retrieval
problem and is referred to in this paper as the Phase
Analytic Technique. The first step in the Phase Analytic
Technique is to represent the aperture wavefront in a
finite Fourier series. Using a known pupil function
(equation (13)) and the representation for the focal plane
wavefront (equation (12)) an expression for the aperture
wavefront is obtained (Ref 9). Now, expanding the aperture
field in a Fourier series

$$P(x_a, y_a) \exp\left(j \, w_a(x_a, y_a)\right) = \sum_{N=-\infty}^{\infty} \sum_{M=-\infty}^{\infty} P(x_a, y_a) \, F_{NM}$$

$$\exp\left(j 2\pi\left(\left(\frac{N}{w_x}\right)x_a + \left(\frac{M}{w_y}\right)y_a\right)\right) \qquad (16)$$

where the (F_{nm}) terms are complex Fourier coefficients.
After substituting the above expansion of the aperture
field (equation (16)) into equation (8) an expression for
the focal plane field is obtained

$$U_f(x_f, y_f) \cong \left(\frac{1}{\lambda f}\right) \mathcal{F}_{xy}\left\{ P(x_a, y_a) \sum_{N=-\infty}^{\infty} \sum_{M=-\infty}^{\infty} F_{NM} \exp\left(j 2\pi\left(\frac{N}{w_x}x_a + \frac{M}{w_y}y_a\right)\right) \right. \qquad (17)$$

After performing the above transform we find the focal
wavefront to be

$$U_f(x_f, y_f) \cong \left(\frac{1}{\lambda f}\right) \sum_{N=-\infty}^{\infty} \sum_{M=-\infty}^{\infty} F_{NM} \frac{SIN\left(\frac{\pi w_x}{\lambda f}\left(x_f + \frac{N\lambda f}{w_x}\right)\right)}{\frac{\pi}{\lambda f}\left(x_f + \frac{N\lambda f}{w_x}\right)} \frac{SIN\left(\frac{\pi w_y}{\lambda f}\left(y_f + \frac{M\lambda f}{w_y}\right)\right)}{\frac{\pi}{\lambda f}\left(y_f + \frac{M\lambda f}{w_y}\right)} \qquad (18)$$

For notational simplicity the sinc function is defined to
be

$$SINC_N x_f = \frac{SIN\left(\frac{\pi w_x}{\lambda f}\left(x_f + \frac{N\lambda f}{w_x}\right)\right)}{\frac{\pi w_x}{\lambda f}\left(x_f + \frac{N\lambda f}{w_x}\right)} \qquad (19)$$

Using this sinc function (equation (19)) equation (18)
simplifies to

14

$$U_f(x_f, y_f) \cong \frac{\omega_x \omega_y}{\lambda f} \sum_{N=-\infty}^{\infty} \sum_{M=-\infty}^{\infty} F_{NM} \, SINC_N X_f \, SINC_M Y_f \qquad (20)$$

Equation (20) forms an orthogonal set of basis functions to represent the focal plane field. From equation (20) an expression for the focal plane intensity is found

$$I_f(x_f, y_f) = \left| \frac{\omega_x \omega_y}{\lambda f} \sum_{N=-\infty}^{\infty} \sum_{M=-\infty}^{\infty} F_{NM} \, SINC_N X_f \, SINC_M Y_f \right|^2 \qquad (21)$$

Now, we have a representation for the focal plane intensity $(I_f(x_f, y_f))$ and we know the exact focal plane intensity $(I_m(x_f, y_f))$, which is a measured quantity. For optimization purposes a method for determining the Fourier series coefficients (F_{nm}) is needed. A cost function (J) is defined to minimize the mean square error between the focal plane intensity representation $(I_f(x_f, y_f))$ and the measured focal plane intensity $(I_m(x_f, y_f))$, specifically

$$J = \int_{-\infty}^{\infty} \int_{-\infty}^{\infty} \left| I_m(x_f, y_f) - I_f(x_f, y_f) \right|^2 dx_f \, dy_f \qquad (22)$$

This cost function (J) is known as the "approximation by the method of least squares or an approximation in the mean" (Ref 10). Expanding equation (22) yields

$$J = \int\int \left| I_m^2(x_f, y_f) + I_f^2(x_f, y_f) - 2 I_f(x_f, y_f) I_m(x_f, y_f) \right| dx_f \, dy_f \qquad (24)$$

After substituting the representation for the focal plane
intensity (equation (21)) into this cost function
(equation (23)), a closed form solution to this optiza-
tion problem could not be found. An excessive number of
cross terms are generated by the representation of the
intensity in the focal plane squared $((I_f(x_f,y_f))^2)$ term.
Specifically

$$I_f^2(x_f,y_f) = \left| \frac{\omega_x \omega_y}{\lambda f} \sum_{N=-\infty}^{\infty} \sum_{M=-\infty}^{\infty} F_{NM} \, SINC_N x_f \, SINC_M y_f \right|^2$$

$$\left| \frac{\omega_x \omega_y}{\lambda f} \sum_{P=-\infty}^{\infty} \sum_{Q=-\infty}^{\infty} F_{PQ} \, SINC_P x_f \, SINC_Q y_f \right|^2 \quad (24)$$

The fact that the representation of the focal plane electric
field is an orthogonal series does not help in this case
since we are dealing with powers of intensity.

Numerical Approaches. An analytical closed form
solution could not be found, so two numerical approaches
were developed. These numerical approaches use the measured
intensity in the focal plane to generate the Fourier series
coefficients. These estimated Fourier series coefficients
are then used to generate an approximated complex aperture
wavefront.

The first numerical approach is the Phase Numeric 1
Technique. This technique uses equation (20) to find an
expression for the Fourier series coefficients, specifi-
cally

$$\int_{-\infty}^{\infty}\int_{-\infty}^{\infty} U_f(x_f,y_f)\, SINC_I^*x_f\, SINC_J^*\, y_f\, dx_f\, dy_f =$$

$$\frac{\omega_x \omega_y}{\lambda f} \int_{-\infty}^{\infty}\int_{-\infty}^{\infty} \sum_{N=-\infty}^{\infty}\sum_{M=-\infty}^{\infty} F_{NM}\, SINC_N x_f\, SINC_M y_f\, SINC_I x_f\, SINC_J y_f\, dx_f\, dy_f \quad (25)$$

Solving equation (25) for the Fourier series coefficients
yields

$$F_{IJ} = \left(\frac{1}{\lambda f}\right) \int_{-\infty}^{\infty}\int_{-\infty}^{\infty} U_f(x_f,y_f)\, SINC_I^*\, x_f\, SINC_J^*\, y_f\, dx_f\, dy_f \quad (26)$$

which is an exact expression for the Fourier series
coefficients. An approximation is made by using the
modulus of the focal plane field (from measured intensity
data) instead of the actual unknown complex electric field
in the focal plane, specifically

$$F_{IJ} = \left(\frac{1}{\lambda f}\right) \int_{-\infty}^{\infty}\int_{-\infty}^{\infty} |U_f(x_f,y_f)|\, SINC_I^*x_f\, SINC_J^*y_f\, dx_f\, dy_f \quad (27)$$

Once the approximated Fourier series coefficients are
calculated they are used to reconstruct the aperture electric
field.

In order to evaluate the validity of the assumption
that the modulus of the focal plane field can be approximate
the complex focal plane field in equation (26) an error
analysis is shown. The expected mean square error (E(error))
between the focal plane electric field and the modulus of the
focal plane field is

$$E[error] = E\left[\int_{-\infty}^{\infty}\int_{-\infty}^{\infty}\Big|\,|U_f(x_f,y_f)| - U_f(x_f,y_f)\,\Big|^2 dx_f dy_f\right] \qquad (28)$$

where

$$U_f(x_f,y_f) = |U_f(x_f,y_f)|\,exp(\jmath\,\phi(x_f,y_f)) \qquad (29)$$

and

$$\phi(x_f,y_f) = \text{phase of the focal plane field}$$

The expected error reduces to

$$E[error] = E\left[\int_{-\infty}^{\infty}\int_{-\infty}^{\infty}|U_f(x_f,y_f)|^2\,\big|1 - exp(-\jmath\,\phi(x_f,y_f))\big|dx_f dy_f\right]$$

$$= 2E\left[\int_{-\infty}^{\infty}\int_{-\infty}^{\infty}|U_f(x_f,y_f)|^2\,\big|1 - cos(\phi(x_f,y_f))\big|dx_f dy_f\right] \qquad (30)$$

The phase of the focal plane field for arbitrary aperture
fields is not known. In order to gain insight into this
error analysis the phase of the focal plane field is modeled
as a Random Guassian Process. It is assumed that the mean
of the aperture phase is zero and the variance is sigma
squared (σ^2).

$$E[\phi(x_f,y_f)] = 0 \qquad (31)$$

18

and

$$E\left[\left(\phi(x_f, y_f)\right)^2\right] = \sigma^2 \tag{32}$$

Note that the expected value of the phase term $(\exp(-j\phi(x_f, y_f)))$ is the definition of the characteristic function, and its expected value is

$$E\left[\exp\left(-j\,\phi(x_f, y_f)\right)\right] = \exp\left(-\tfrac{1}{2}\sigma^2\right) \tag{33}$$

The expected value of the cosine term in equation (30) is

$$E\left[\cos\left(\phi(x_f, y_f)\right)\right] = Re\left[\exp\left(-\tfrac{1}{2}\sigma^2\right)\right] \tag{34}$$

So, the expected mean square error between the focal plane electric field and its modulus from this model (Random Gaussian Process) is

$$E\left[error\right] = 2\int_{-\infty}^{\infty}\int_{-\infty}^{\infty} \left|U_f(x_f, y_f)\right|^2$$
$$\left|1 - Re\left[\exp\left(-\tfrac{1}{2}\sigma^2\right)\right]\right| dx_f\, dy_f \tag{35}$$

There is no reason to believe that the variance of the focal plane phase is small (actually it is expected to be large) the expected mean square error for this model is

$$E[error] = \alpha \int_{-\infty}^{\infty} \int_{-\infty}^{\infty} |U_f(x_f, y_f)|^2 \, dx_f \, dy_f \qquad (36)$$

From this error analysis the Phase Numeric 1 Technique is not expected to be a good signal processing technique for the retrieval of the aperture phase from intensity data in the focal plane (Refs 11 and 12).

The second numerical approach, developed from the Phase Analytic Technique, to determine the spatial (relative) phase of the aperture field is called the Phase Numeric 2 Technique. This technique is a brute force method using an International Mathematical Statistical Library (IMSL) sub-routine ZXMIN to estimate the complex Fourier series coefficients (Ref 13). These Fourier series coefficients are then used to reconstruct the aperture field. This technique is developed in this paper for an aperture field which is a function of one spatial variable (one-dimensional fields). This analysis can be expanded for two-dimensional fields.

The subroutine ZXMIN minimizes a user supplied function of N variables using a quasi-Newton method (Ref 14). The user supplied subroutine is a cost function which first uses the N variables ($c(N)$) estimated by ZXMIN to form Fourier series coefficients in rectangular (case a) and polar (case b) coordinates, specifically, case a

$$\widehat{FN\,RECT}_I = C(I) + j\,C\left(I + \tfrac{N}{2}\right) \tag{37}$$

and case b

$$\widehat{FN\,POLAR}_I = C(I)\,exp\left(j\,C\left(I + \tfrac{N}{2}\right)\right) \tag{38}$$

These Fourier series coefficients are then used to approximate the focal plane wavefront

$$\widehat{U}_f(X_f) = \sum_{I=-\infty}^{\infty} \widehat{FN}_I\,exp\left(\frac{j\,2\pi\,I\,X_f}{\omega_x}\right) \tag{39}$$

The cost function is then generated point by point

$$J = \sum_{\substack{I \\ across \\ detector}} \left| I_M(I) - \widehat{I}_f(I) \right|^2 \tag{40}$$

where

$I_m(I)$ = measured focal plane intensity at point I

$\widehat{I}_f(I)$ = calculated focal plane intensity from the approximated Fourier series coefficients at point I

and

$$\widehat{I}_f(I) = \left| U_f(I) \right|^2 \tag{41}$$

The IMSL subroutine ZXMIN iterates varying the N variables

(Fourier coefficients) minimizing the cost funct (J), as defined in equation (40). For a more thorough explanation of the IMSL subroutine ZXMIN refer to reference 14, "Fortran Subroutines for Minimization by Quasi-Newton Methods", by R. Fletcher.

The number of Fourier series coefficients calculated are N/2 since these coefficients have real and imaginary parts. Once the optimized Fourier series coefficients are determined the aperture wavefront can be computed by inverse Fourier transforming the optimized focal plane field.

This technique is similar to one tried by W.H. Southwell (Ref 6), where Zernike circle polynomials are used to approximate the phase of the aperture field instead of the Fourier series expansion method used in this research study.

Autocorrelation Function. In order to decrease the number of variables that have to be optimized using the Phase Numeric 2 Technique, the autocorrelation function of the aperture field was investigated. The reasoning is that the use of more of the available information could result in the reduction of computational time and could improve the convergence properties of the Phase Numeric 2 Technique. This technique is developed in this report for aperture fields which are a function of one spatial variation (one-dimensional fields).

The autocorrelation function $(R(\Delta x))$ of the aperture field is

$$R(\Delta x) = \mathcal{F}_x^{-1}\left\{\left|\ \mathcal{F}_x\ \left\{U_a(x_a)\right\}\right|^2\right\} \tag{42}$$

The Fourier transform of the aperture field squared $((\mathcal{F}(U_a(x_a,y_a)))^2)$ in the focal plane is a measured quantity within a known constant, specifically

$$R(\Delta x) = \mathcal{F}_x^{-1}\left\{\ (\lambda f)\ I_M(x_f)\right\} \tag{43}$$

The auto correlation theorem states that if $g(x)$ and $G(f)$ are Fourier transform pairs then

$$\mathcal{F}\left\{\int_{-\infty}^{\infty} g(\xi)\ g^*(\xi - x)\ d\xi\right\} = |G(f)|^2 \tag{44}$$

(Ref 9). Using the representation for the aperture wavefront in equation (12) and equation (16) then substituting in the autocorrelation theorem (equation (44)) we find

$$R(\Delta x) = \frac{1}{\omega_x}\int_{-\frac{\omega_x}{2}}^{\frac{\omega_x}{2}} \sum_{N=-\infty}^{\infty} \sum_{M=-\infty}^{\infty} F_N F_M^* \exp\left(\frac{j2\pi N}{\omega_x} x_a\right)$$
$$\exp\left(\frac{-j2\pi M}{\omega_x}(x_a - \Delta x)\right) dx \tag{45}$$

After preforming the integration in equation (45) the above autocorrelation function (equation (45)) reduces to

$$R(\Delta x) = \sum_{N=-\infty}^{\infty} |F_N|^2 \exp\left(j\frac{2\pi N}{\omega x}\Delta x\right) \tag{46}$$

From equation (46) the magnitude of the Fourier series coefficients squared be found

$$|F_N|^2 = \frac{1}{2W} \sum_{\Delta x=-W}^{W} R(\Delta x)\exp\left(-j\frac{\pi N}{\omega x}\Delta x\right) \tag{47}$$

specifically

$$|F_N|^2 = \frac{1}{2W} \sum_{\Delta x=-W}^{W} \mathcal{F}_x^{-1}\left\{(\lambda f)I_M(\Delta x)\right\}$$
$$\exp\left(-j\frac{\pi N}{\omega x}\Delta x\right) \tag{48}$$

Equation (48) is a direct method to compute the magnitude
of the Fourier series coefficients which can be used in
the Phase Numeric 2 Technique. Using this result only
N phase terms have to be optimized for N Fourier series
coefficients.

Gerchberg-Saxton Algorithm

The Gerchberg-Saxton Algorithm is an iterative method
developed to solve the phase retrieval problem in electron
microscopy (Ref 7). Adapted to solve the imaging sensor
phase retrieval problem the Gerchberg-Saxton Algorithm
(Fig 4) starts with an initial guess of the aperture wave-
front ($\hat{f}_{a1}(x_a)$). The approximated focal plane wavefront

$(\hat{F}_1(x_f))$ is the Fourier transform of the initial guess of
the aperture wavefront

$$\hat{F}_1(x_f) = \mathcal{F}_x \left\{ \hat{f}_{a1}(x_a) \right\} \qquad (49)$$

This approximated focal plane wavefront is then modified by
dividing it by its modulus (normalizing intensity) and then
multiplying this function by the measured modulus in the
focal plane $((I_m(x_f))^{\frac{1}{2}})$

$$\hat{F}_2(x_f) = \frac{\hat{F}_1(x_f)}{|\hat{F}_1(x_f)|} \left(I_M(x_f) \right)^{1/2} \qquad (50)$$

This new focal plane wavefront $(\hat{F}_2(x_f))$ has the modulus of
the measured focal plane wavefront and a phase which is a
function of the initial guess of the aperture wavefront
$(\hat{f}_{a1}(x_a))$. Now, the approximated aperture plane field
$(\hat{f}_{a2}(x_a))$ is the inverse Fourier transform of the modified
focal plane field $(\hat{F}_2(x_f))$

$$\hat{f}_{a2}(x_a) = \mathcal{F}_x^{-1} \left\{ \hat{F}_2(x_f) \right\} \qquad (51)$$

This approximated aperture plane field $(\hat{f}_{a2}(x_a))$ is the
output of the Gerchberg-Saxton Algorithm and is a function
of the initial guess of the aperture wavefront $(\hat{f}_{a1}(x_a))$
and the intensity measurement $(I_m(x_f))$ in the focal plane
of the imaging sensor. The output of the first iteration

25
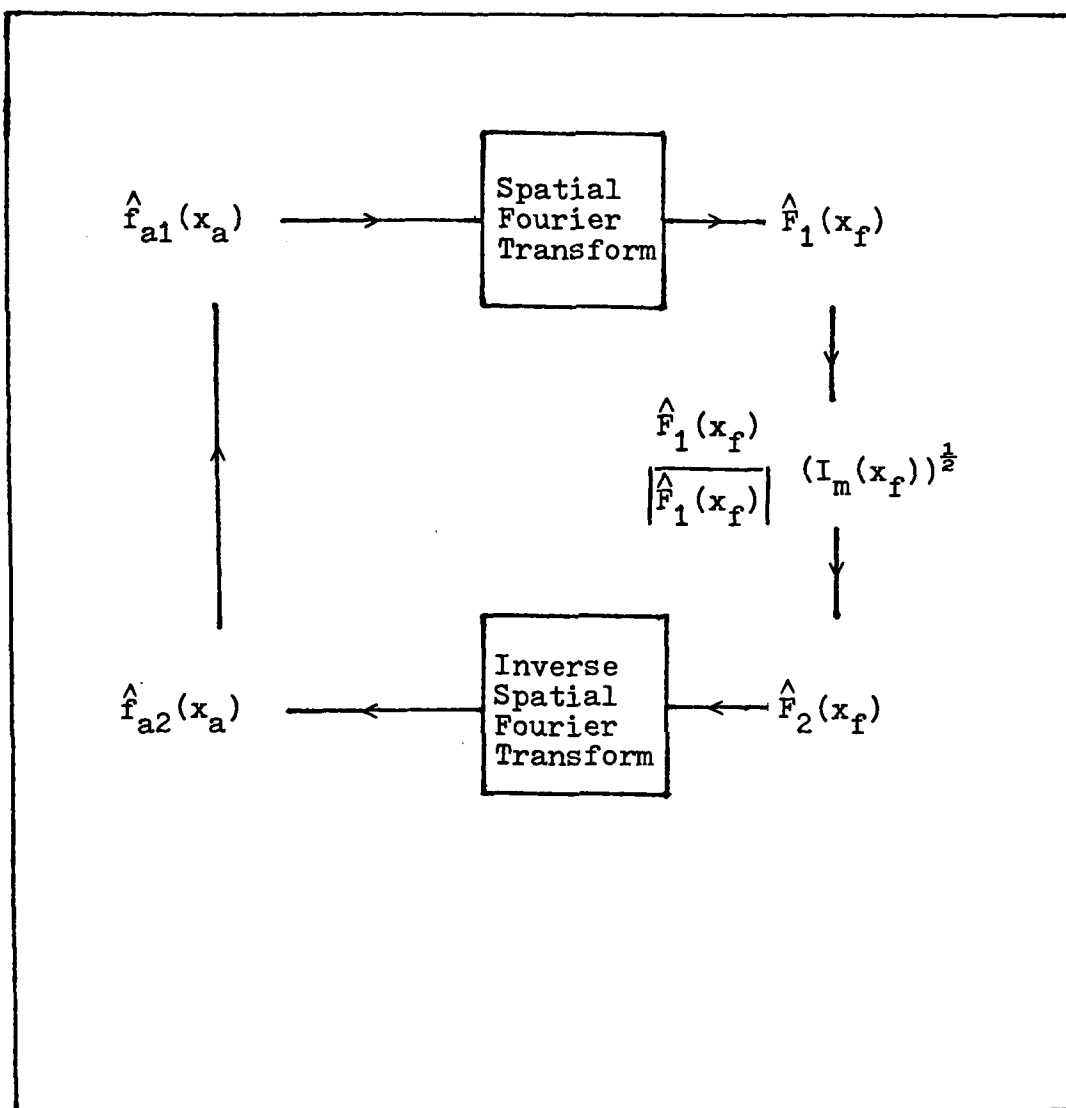
Figure 4. Block diagram of the Gerchberg-Saxton Algorithm

$(\hat{f}_{a2}(x_a))$, is now used as the new guess of the aperture wavefront $(\hat{f}'_{a1}(x_a))$. This procedure is continued until convergence or the desired accuracy is achieved.

Error Reduction Technique. J.R. Fienup modified the Gerchberg-Saxton Algorithm with an input/output technique which is called the "Error Reduction Technique". This technique yields a solution which improves with each iteration, reducing the mean square error between the focal plane intensities (calculated versus measured), thus the name Error Reduction Technique. Instead of using the output estimate of the aperture field $(\hat{f}_{a2}(x_a))$ directly as the next guess of the aperture plane field $(\hat{f}'_{a1}(x_a))$ and continue to iterate (Fig 5), J.R. Fienup uses $\hat{f}_{a1}(x_a)$, $\hat{f}_{a2}(x_a)$, object constraints, and feedback techniques to compute the new aperture field guess $(\hat{f}'_{a1}(x_a))$, and then iterates (Ref 8).

With the Error Reduction Technique in mind, two feedback techniques are postulated that use object constraints that are related to the retrieval of the phase of the aperture field from intensity measurements in the focal plane problem that is being addressed by this research study (Fig 5). The object constraints that are used for this project are that the wavefront being approximated must have a modulus of one across the aperture and zero elsewhere.

The first feedback technique postulated is when the output aperture field $(\hat{f}_{a2}(x_a))$ approximated satisfies

27

$(\hat{f}_{a2}(x_a))$, is now used as the new guess of the aperture wavefront $(\hat{f}'_{a1}(x_a))$. This procedure is continued until convergence or the desired accuracy is achieved.

Error Reduction Technique. J.R. Fienup modified the Gerchberg-Saxton Algorithm with an input/output technique which is called the "Error Reduction Technique". This technique yields a solution which improves with each iteration, reducing the mean square error between the focal plane intensities (calculated versus measured), thus the name Error Reduction Technique. Instead of using the output estimate of the aperture field $(\hat{f}_{a2}(x_a))$ directly as the next guess of the aperture plane field $(\hat{f}'_{a1}(x_a))$ and continue to iterate (Fig 5), J.R. Fienup uses $\hat{f}_{a1}(x_a)$, $\hat{f}_{a2}(x_a)$, object constraints, and feedback techniques to compute the new aperture field guess $(\hat{f}'_{a1}(x_a))$, and then iterates (Ref 8).

With the Error Reduction Technique in mind, two feedback techniques are postulated that use object constraints that are related to the retrieval of the phase of the aperture field from intensity measurements in the focal plane problem that is being addressed by this research study (Fig 5). The object constraints that are used for this project are that the wavefront being approximated must have a modulus of one across the aperture and zero elsewhere.

The first feedback technique postulated is when the output aperture field $(\hat{f}_{a2}(x_a))$ approximated satisfies

Figure 5. Gerchberg-Saxton Algorithm with object constraints controlling feedback

the object constraints, the aperture field ($\hat{f}_{a1}(x_a)$) pixel
(realization at point x_a) stays the same. If the output
aperture field approximation ($\hat{f}_{a2}(x_a)$) does not satisfy
the object constraints, feedback is used to compute the
aperture pixel ($\hat{f}'_{a1}(x_a)$), specifically

$$\hat{f}'_{a1}(x_a) = \begin{cases} \hat{f}_{a1}(x_a) & ; \text{ if } \hat{f}_{a2}(x_a) \text{ SATISFIES OBJECT CONSTRAINTS} \\ \hat{f}_{a1}(x_a) - \beta \hat{f}_{a2}(x_a) ; & else \end{cases} \quad (52)$$

Beta is a feedback operator and is defined in chapter
four, "Simulation Results and Analysis".

The second feedback technique postulated differs from
the first feedback technique in that the estimated aperture
wavefront is always zero outside the aperture. When the
output aperture field approximation ($\hat{f}_{a2}(x_a)$) satisfies the
object constraints, the aperture pixel ($\hat{f}_{a1}(x_a)$) stays the
same. If the output aperture field approximation ($\hat{f}_{a2}(x_a)$)
does not satisfy the object constraints, feedback is used to
compute the aperture pixel ($\hat{f}'_{a1}(x_a)$). The addition constraint
is that if the aperture field outside the aperture is not
zero it is set to zero, specifically

$$\hat{f}'_{a1}(x_a) = \begin{cases} 0 & ; \text{ OUTSIDE APERTURE} \\ \hat{f}_{a1}(x_a) & , \text{ if } \hat{f}_{a2}(x_a) \text{ SATISFIES} \\ & ; \text{ OBJECT CONSTRAINTS} \quad (53) \\ \hat{f}_{a1}(x_a) - \beta \hat{f}_{a2}(x_a) ; & else \end{cases}$$

The best feature of the Gerchberg-Saxton Algorithm is that the Fourier series coefficients are not computed, eliminating the errors that are inevitable whenever a series representation is artifically truncated.

In this chapter, the phase retrieval techniques investigated in this research project were developed. The first approach undertaken is addressed at finding an analytical solution to the phase retrieval problem. When a closed form solution could not be found to this approach two numerical techniques were developed. The Phase Numeric 1 Technique used analytical results from the Phase Analytic Technique and the assumption that the focal plane field can be approximated by the modulus of the focal plane field in order to retrieve the phase of the aperture wavefront. The Phase Numeric 2 Technique also used analytical results from the Phase Analytic Technique and a parameter optimization subroutine to approximate the Fourier series coefficients. These Fourier series coefficients are then used to infer the phase of the aperture field. The second approach investigated to retrieve the phase of the aperture field is based on the Gerchberg-Saxton Algorithm. The Gerchberg -Saxton Algorithm and two feedback techniques are developed which directly retrieve the aperture phase.

IV Simulation Results and Analysis

The previous chapter developed various techniques directed at solving the phase retrieval problem. This chapter defines the aperture wavefronts used in the simulations, the measure of performance, and presents the data and performance analysis of the phase retrieval techniques that are simulated. The techniques simulated are: the Phase Numeric 1 Technique, Phase Numeric 2 Technique, and the Gerchberg-Saxton Algorithm with and without feedback.

Aperture Wavefronts

The phase retrieval techniques studied in this project were simulated as a function of one spatial variation (one-dimensional fields). The aperture field consists of 15 sampled pixels (across the aperture) and the focal plane consists of 32 pixels. The aperture wavefronts that are used for the simulations are complex with a modulus of one

$$f_a(x_a) = exp\left(j\,\omega_a(x_a)\right) \tag{54}$$

The wavefront functions simulated are: a constant term (a trivial case), a linear term (tilt), a sine term (odd function), a cosine term (even function) and a random term which is linearly distributed between zero and one.

Figure 5 illustrates the relative (spatial) phase ($w_a(x_a)$) across the aperture for the linear, sine and cosine wavefronts. The trivial constant phase term is not shown. Figure 6 illustrates the random1(x_a) and the random2(x_a) distributions used in the simulations.

<u>Performance Measures</u>

In order to compare the performance of the simulated phase retrieval techniques the mean square error between the phase of the aperture wavefront and the estimated wavefront is used

$$MSE = \sum_{\substack{L \\ across \\ aperture}} \left(| w_a(L) - \hat{w}_a(L)|^2 \right) \tag{55}$$

where

$w_a(L)$ = phase of the aperture wavefront at pixel L

$\hat{w}_a(L)$ = phase of the approximated aperture wavefront at pixel L

Now, in order to compare the relative accuracy of the simulated phase retrieval methods with various aperture wavefronts, a normalized mean square error is used

$$NMSE = \frac{\sum_L | w_a(L) - \hat{w}_a(L)|^2}{\sum_{\substack{L \\ across\ aperture}} | w_a(L)|^2} \tag{56}$$

In the case where the denominator in equation (56) is equal

32
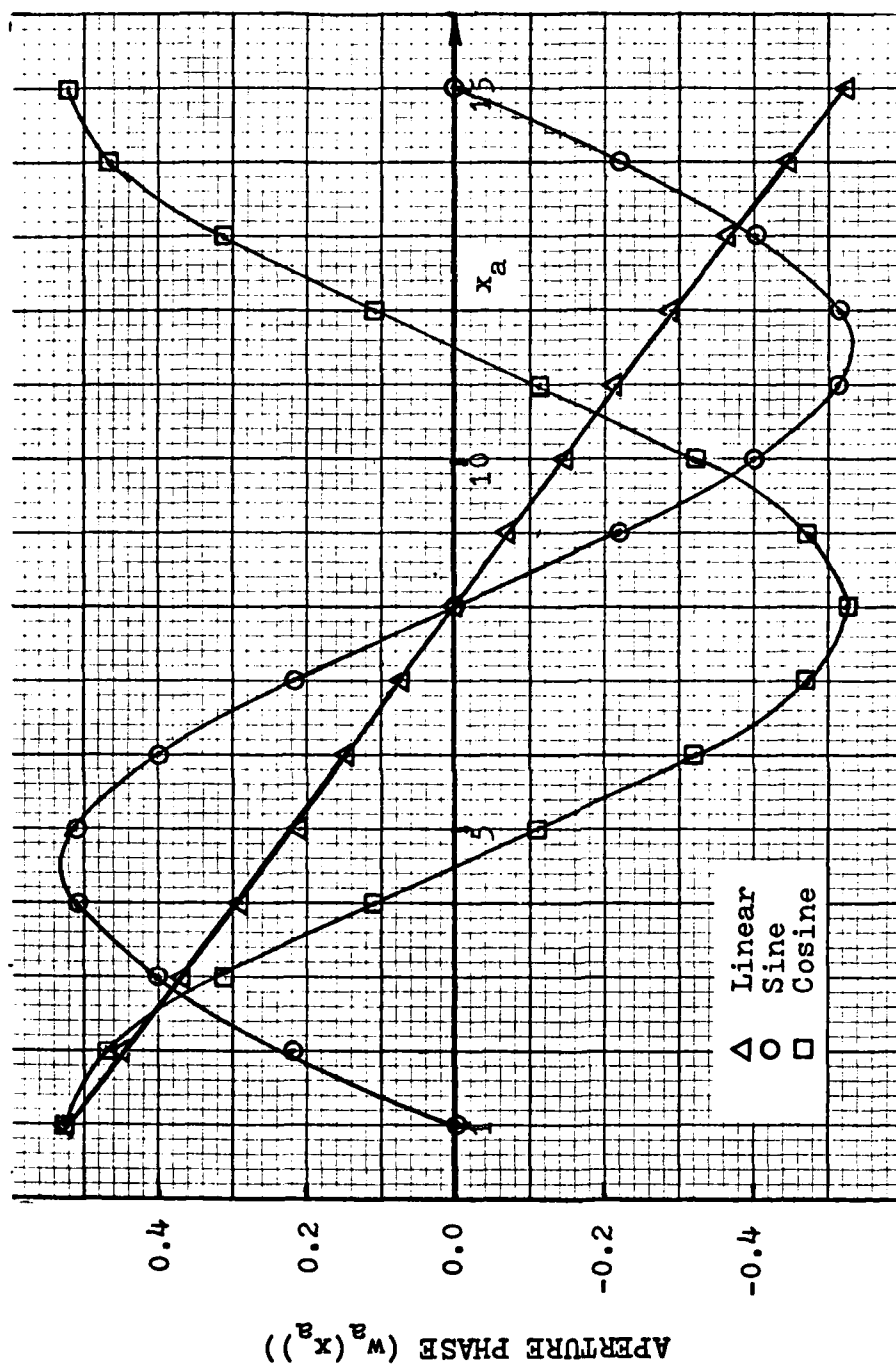
Figure 6. Relative aperture phase test cases

33
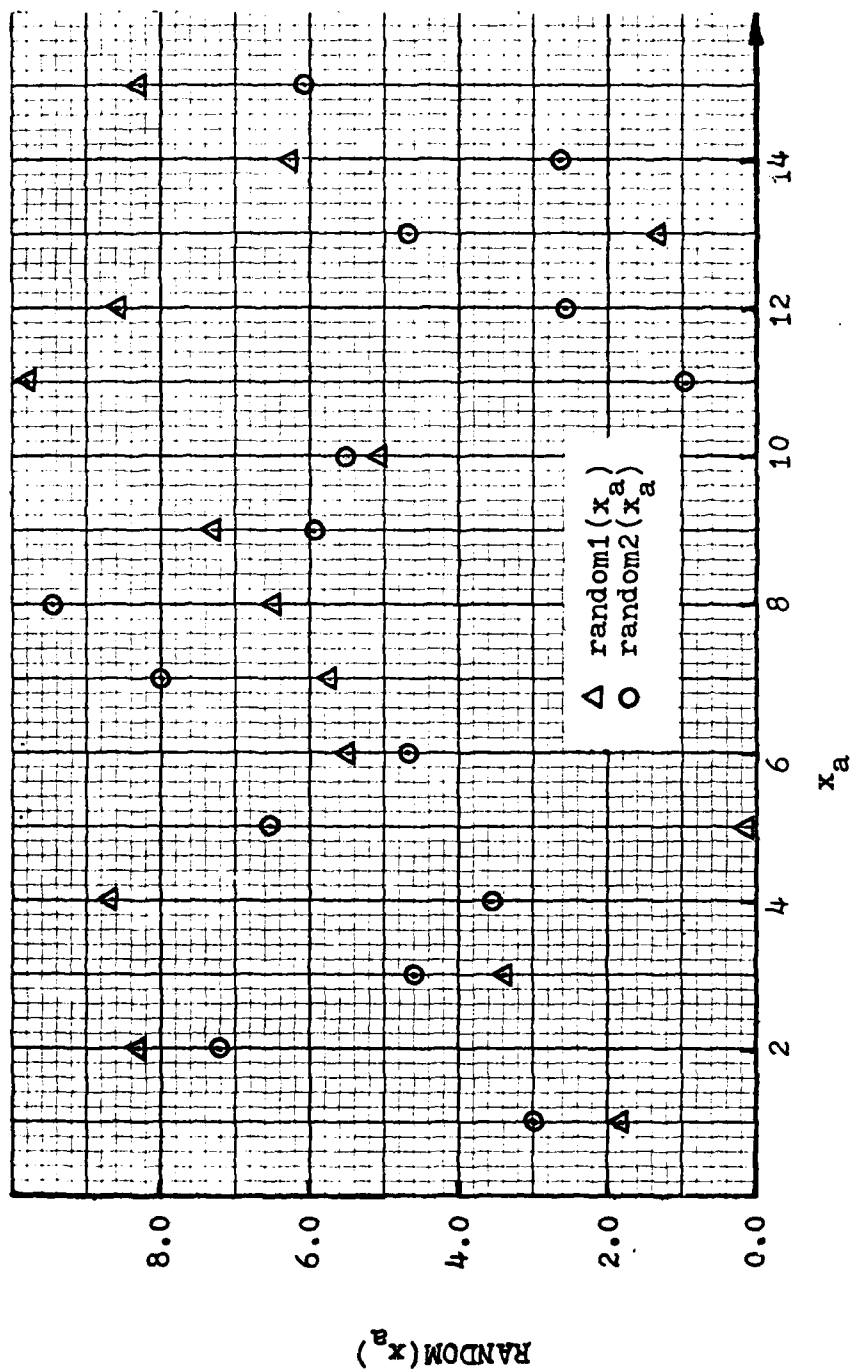
Figure 7. Random number distribution

to zero, the denominator is set to one (this occurs when the phase of the aperture wavefront is exactly zero across the aperture).

Phase Numeric Approaches

The phase numeric approaches use the measured intensity in the focal plane to generate the Fourier series coefficients of the aperture wavefront. These approximated Fourier series coefficients are then used to retrieve the phase of the aperture wavefront.

Phase Numeric 1 Technique. The Phase Numeric 1 Technique makes use of the orthogonal set of basis functions found in the Phase Analytic Approach to generate the Fourier series coefficients. The Fourier series coefficients that are computed from simulating this technique are not acceptable. The Phase Numeric 1 Technique worked well on the computation of the $\hat{F}_0$ coefficient, but the higher order Fourier series coefficients computed had unsystematic errors which are attributed to the approximation that the magnitude of the focal plane field can be used in equation (27) for the complex focal plane field. The error analysis, on pages 17, 18, and 19 , indicate that the above approximation is a poor one and the simulations prove it is a poor one.

Phase Numeric 2 Technique. The Phase Numeric 2 Technique is a brute force method using an IMSL subroutine (Ref 13) to optimize the complex Fourier series coefficients by minimizing the mean square error between the focal plane intensity measured and the focal plane intensity calculated.

For N/2 Fourier series coefficients there are N real variables
which have to be optimized, since the Fourier series coeffi-
cients are complex. These Fourier series coefficients are
calculated in rectangular (FNRECT, case 1), and then in
Polar (FNPOLAR, case 2) coordinates. The number of Fourier
series coefficients (#FN's) are varied between one ($\hat{F}_0$) and
nine ($\hat{F}_0$, $\hat{F}_{\pm 1}$, $\hat{F}_{\pm 2}$, $\hat{F}_{\pm 3}$, and $\hat{F}_{\pm 4}$). Table 1 lists the best
(least NMSE) versus the worst (largest NMSE) performance
of the Phase Numeric 2 Technique for the Fourier series
coefficients computed simultaneously. It is interesting
to note that the worst performance was achieved for the
number of Fourier series coefficients equal to three or
seven, while the best performance was achieved with the
number of Fourier series coefficients equal to five (except
for one in the trivial constant phase case). There does not
seem to be much difference in Normalized Mean Square Error
(NMSE) or the iterations (ITT) required when the Fourier
series coefficients are computed in polar or in rectangular
coordinates. Note that computation (iterations) are
stopped when the approximated Fourier series coefficients
are not changed (three significant figures) by the Phase
Numeric 2 Technique subroutine ZXMIN for two consecutive
iterations or on the 1000 iteration, whichever occurs
first. The average execution time is 0.025cp execution
seconds per iteration, and with the routine often requiring
the full 1000 iterations allowed (and still not totally
converging to a solution) equates to 250cp execution

36

Aperture	FNRECT			FNPOLAR		
Phase	NMSE	#FN's	ITT	NMSE	#FN's	ITT
1. Const	0.0	1	13	0.0	1	13
	1.7E-2	7	1000	6.0E-10	7	1000
2. Linear	2.2E-1	5	614	2.3E-1	5	1000
	3.4	7	1000	3.0E-1	3	465
3. Sine	9.8E-1	5	1000	9.8E-1	5	920
	1.6	3	250	1.5	3	290
4. Cosine	9.9E-1	5	530	8.3E-1	5	1000
	1.0	3	224	1.0	7	1000

Table 1. Representative Simulation Results - Best vs. Worst
Performance for the Phase Numeric 2 Technique (Simultaneously)

seconds.

This technique did a fair job in approximating the
linear phase aberation (NMSE = 0.2) and zero phase (NMSE =
1E-2) but had unacceptable performance for the cosine and
the sine (NMSE = 1) phase aberations. Increasing the
number of Fourier series coefficients should improve the
accuracy achievable, the problem is that as the number of
variables that have to be optimized is increased convergence
is more difficult to achieve (while increasing round off errors
in the IMSL subroutine ZXMIN).

In an attempt to increase the number of Fourier series
coefficients without increasing the number of variables being
optimized, at any one time, the Fourier series coefficients
were computed serially, first $\hat{F}_0$, then $\hat{F}_{\pm 1}$ and so on. Table
2 lists representative simulation results showing best (least
NMSE) and worst (highest NMSE) for the aperture wavefronts
indicated. It is interesting to note that the NMSE with
nine Fourier series coefficients were either the best or the
worst simulation cases for seven out ot the eight cases
shown. This technique of computing the Fourier series coeffi-
cients serially yielded similar results to the technique
where the Fourier series coefficients were computed simul-
taneously. Note again that optimization is stopped when
the approximated Fourier series coefficients do not change
(three significant figures) for two consecutive iterations
or on the 1000 iteration (per set of coefficients being
optimized), whichever occurs first. This technique does

38

Aperture Phase	FNRECT			FNPOLAR		
	NMSE	#FN's	ITT	NMSE	#FN's	ITT
1. Const	2.1E-37	1	13	2.1E-27	1	13
	5.0E-10	3	447	1.7E-18	9	643
2. Linear	4.3E-1	9	815	3.8E-1	9	1064
	4.9E-1	3	321	4.4E-1	3	258
3. Sine	1.0	1	66	1.0	1	59
	1.6	9	742	1.6	9	984
4. Cosine	1.0	1	75	1.0	1	58
	1.0	9	768	5.1	9	929

Table 2. Representative Simulation Results - Best vs. Worst Performance for the Phase Numeric 2 Technique (Serially)

a fair job in the approximation of the linear phase function and a good job of approximating the trivial zero phase test case. This technique did an unacceptable job in approximating the sine and cosine aberation cases.

The problem with computing the coefficients serially is that errors are compounded, specifically the error in the $\hat{F}_0$ coefficient causes errors in the optimization of the $\hat{F}_{\pm 1}$ coefficient and so on. The data indicates that if the number of Fourier series coefficients computed is increased beyond the nine computed, the performance of the linear aberation phase retrieval will be increased, since the best performance was achieved when the maximum number of Fourier coefficients (nine) were used. The average execution time is 0.025cp execution seconds per iteration.

To summarize, the Phase Numeric 2 Technique is a fair method to compute linear phase. Figure 8 illustrates and compares the best cases for linear phase retrieval; FNRECT (#FN's are five) for Fourier series coefficients that are computed simultaneously and FNPOLAR (#FN's are nine) for Fourier series coefficients that are computed serially. The NMSE comparisons and Figure 8 indicate that it is better to compute the Fourier series coefficients simultaneously, rather than serially.

Autocorrelation Function. Several computer simulation runs were made, using the autocorrelation function to approximate the magnitude of the Fourier series coefficients and the Phase Numeric 2 Technique to optimize the phase of

40
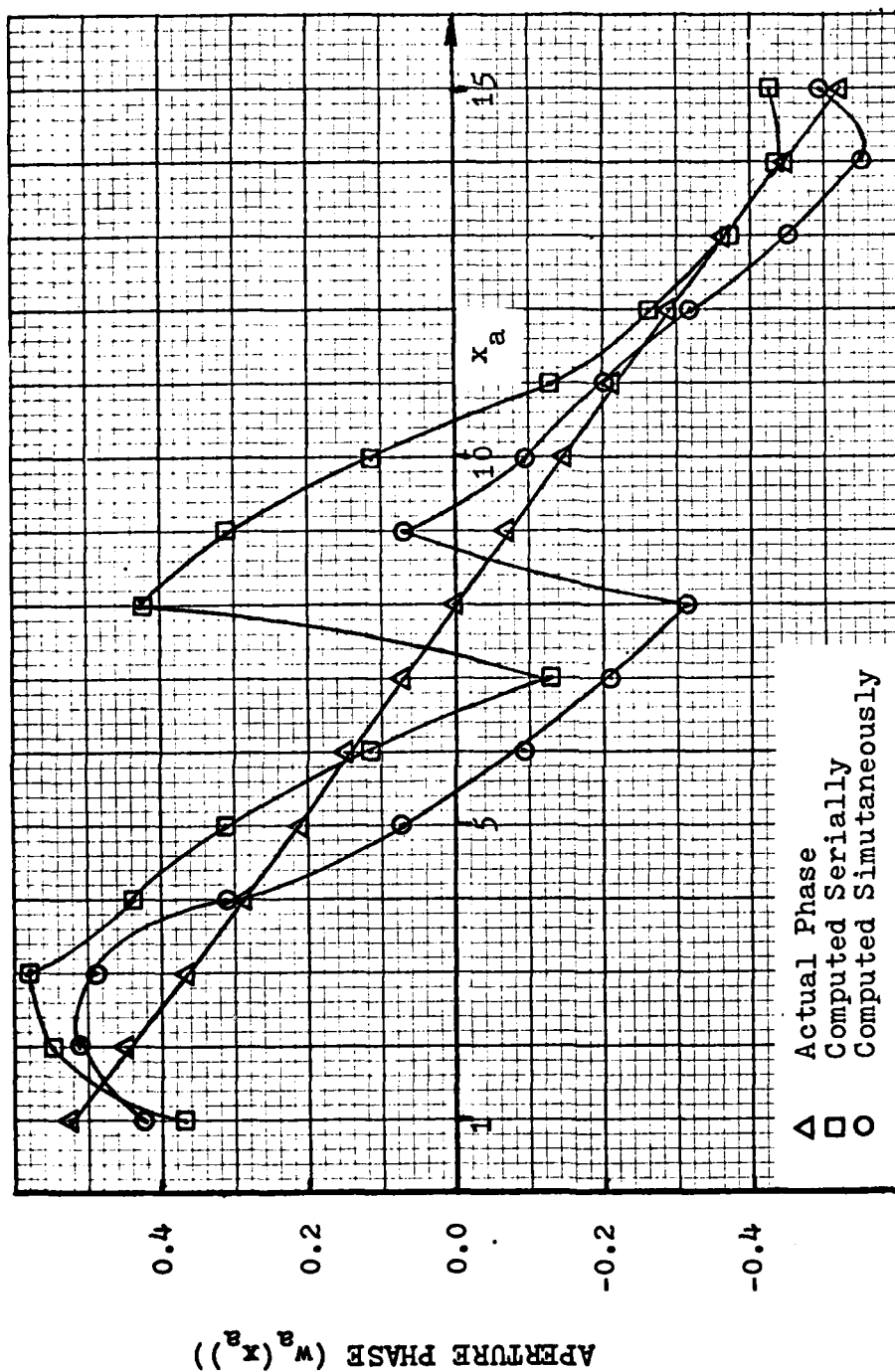
Figure 8. Linear phase reconstruction comparison

Actual Phase △
Computed Serially □
Computed Simultaneously ○

APERTURE PHASE $(W_a(x_a))$

x_a

41

these Fourier series coefficients. In every case tried the magnitude of the $\hat{F}_0$ coefficient is exact, while the higher order Fourier series coefficients had errors in them. These errors caused the Phase Numeric 2 Technique to have convergence problems. The NMSE was one only when the $\hat{F}_0$ coefficient was used to reconstruct the aperture wavefront, and always greater than one when the higher order Fourier series coefficients were used to reconstruct the aperture wavefront.

The analytical solution using the autocorrelation function is exact. The problem with the computation of the magnitude of the Fourier series coefficients is in the numerical technique used. The width of Δx in equation (47) was varied from 1 to 1000 per pixel and it was found that the higher order Fourier series coefficients are very sensitive to the width of Δx, indicating that this is where the numerical problem is. Additional debugging was stopped because of lack of time.

Gerchberg-Saxton Algorithm

The data from the Gerchberg-Saxton Algorithm simulations indicate that it has good convergence properties. The Gerchberg-Saxton Algorithm (without feedback) had the lowest average normalized mean square error (NMSE) and the fastest convergence of the techniques simulated. The Gerchberg-Saxton Algorithm with the first feedback technique had poor performance, never converging to a solution with the normalized mean square error fluctuating on every

42

iteration. The Gerchberg-Saxton Algorithm with the second feedback technique had a low average normalized mean square error and did not converge as quickly as the technique without feedback.

Gerchberg-Saxton Algorithm (without feedback). The Gerchberg-Saxton Algorithm has good convergence properties. Table 3 contains the simulation results of the Gerchberg -Saxton Algorithm. The initial guess of the aperture field $(\hat{f}_{a1}(x_a))$ simulated are: (1) $1 + j0$, and (2) $1 + j\text{random}(x_a)$. The distribution of the random function is shown in Figure 6. The simulation results indicate that the better the initial guess of the aperture field is the better the normalized mean square error (NMSE) of the solution is and the faster the algorithm converges. The actual performance of the algorithm is better than Table 3 indicates in certain cases (note 1). In the cases of the Linear and the Cosine aperture phase aberations the approximated aperture field has bias errors. Figure 9 compares the phase of the aperture field with the Cosine aperture phase aberation to the approximated aperture phase using the Gerchberg-Saxton Algorithm, the bias error is apparent. These bias errors are unimportant since this research is interested in retrieving the relative (spatial) phase of the aperture field. In these cases, when the bias errors are removed, the normalized mean square error is at least one order of magnitude better than indicated.

Aperture Phase	NMSE	#ITT	Init guess of Aperture Field
1. Const	3.8E-29	1	$1+j0$
	9.5E-3	1	$1+j\text{random1}(x_a)/10$
2. Linear	1.7E-2	1	$1+j0$
	1.8E-27	3	$1+j0$
	5.4E-2	1	$1+j\text{random1}(x_a)/10$
	3.7E-2	5	$1+j\text{random1}(x_a)/10$
	3.6E-2	10	$1+j\text{random1}(x_a)/10$
(note 1)	3.4E-2	50	$1+j\text{random1}(x_a)/10$
3. Sine	7.0E-2	1	$1+j0$
	1.6E-27	3	$1+j0$
	1.0	1	$1+j\text{random1}(x_a)/10$
	9.1E-2	10	$1+j\text{random1}(x_a)/10$
4. Cosine	1	1	$1+j0$
	9.6E-2(*)	1	$1+j\text{random1}(x_a)/10$
(note 1)	3.0E-2(*)	2	$1+j\text{random1}(x_a)/10$
5. Random1$(x_a)/10$	8.8E-1	1	$1+j\text{random2}(x_a)/10$
	1.6E-1	8	$1+j\text{random2}(x_a)/10$
6. Random1(x_a)	8.0E-1	1	$1+j\text{random2}(x_a)/10$
	7.9E-1	2	$1+j\text{random2}(x_a)/10$
	9.3E-1	5	$1+j\text{random2}(x_a)/10$
	9.8E-1	10	$1+j\text{random2}(x_a)/10$

(*) indicates convergence to the conjugate
(note 1) indicates bias errors, NMSE is at least one order of magnitude better

Table 3. Simulation Results - Gerchberg-Saxton Algorithm
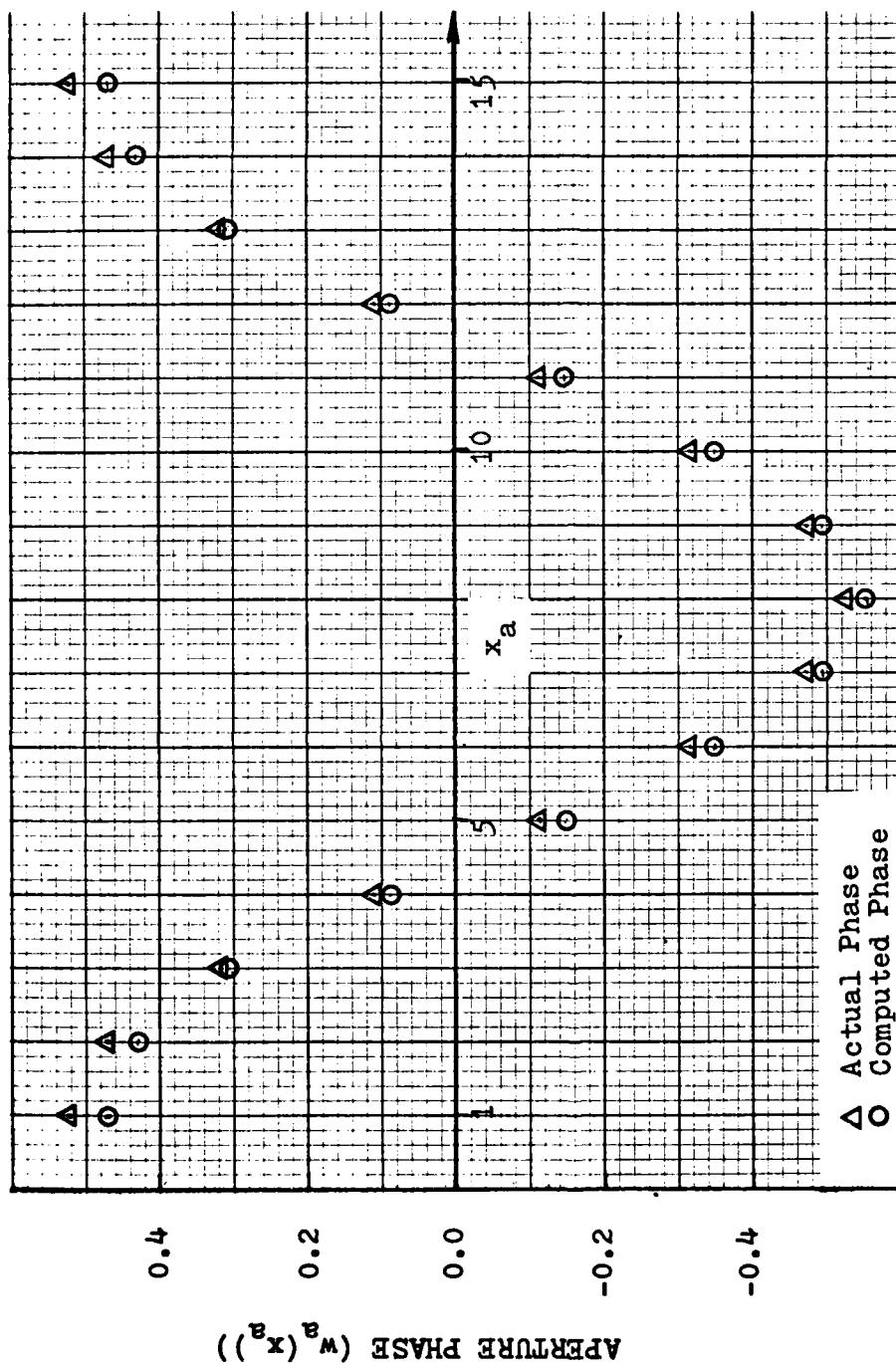
Figure 9. Cosine phase reconstruction comparison

45

In the cases when the aperture phase aberation is an odd function, the algorithm converges to the conjugated aperture phase, while in all other cases the algorithm converges to the actual phase (not conjugated). The literature indicates that this non-uniqueness is not a problem in aperture phase retrieval when the aperture field is a function of two spatial variations (Ref 8). The simulations performed indicate that this technique converges very quickly for the first few iterations and then slows down for the remaining iterations. The Linear aperture phase aberation (Table 3, case 2) with the 1 + jrandom1(x_a) initial guess of the aperture field is a good example of this characteristic; after the first iteration (ITT) the normalized mean square error is 5.4E-2, after the fifth iteration the normalized mean square error is 3.7E-2, and after fifty iterations the normalized mean square error is 3.4E-2. The Gerchberg-Saxton Algorithm converges to a good solution, with a normalized mean square error less than 1.6E-1, in less than 10 iterations for all cases simulated except for the Cosine (case 4) as an aperture phase aberation with the initial guess of the aperture field of 1 + j0, and the Random1(x_a) phase aberation. The Gerchberg -Saxton Algorithm is an excellent technique to estimate Linear, Sine, and Cosine aperture phase aberations, and works well for small random aperture phase functions (Table 3, case 5). This technique requires 0.015cp execution seconds per iteration. If it is estimated that

that 10 iterations are required for convergence, then 0.15cp
execution seconds are needed.

Gerchberg-Saxton Algorithm with Feedback. The
Gerchberg-Saxton Algorithm with feedback techniques use
$\hat{f}_{a1}(x_a)$, $\hat{f}_{a2}(x_a)$, object constraints, and feedback methods
to estimate the next aperture field guess $(\hat{f}'_{a1}(x_a))$ as a
modification to the Gerchberg-Saxton Algorithm.

The first feedback technique simulated uses feedback
whenever (inside and outside toe aperture) the object
constraints are violated. The feedback forms simulated
are

$$\beta \hat{f}_{a2}(x_a) = \begin{cases} fb(s(x_a) + j\, t(x_a) & ; FB_1 \\ fb(s(x_a)) & ; FB_2 \\ fb(t(x_a)) & ; FB_3 \\ fb(j\, s(x_a)) & ; FB_4 \\ fb(j\, t(x_a)) & ; FB_5 \end{cases} \qquad (57)$$

The output aperture field is

$$\hat{f}_{a2}(x_a) = s(x_a) + j\, t(x_a) \qquad (58)$$

The feedback coefficient (fb) is a real constant. The
initial guess of the aperture field is either 1 + j0 across
the aperture and zero elsewhere, or 1 + jrandom(x_a) across
the aperture and zero elsewhere.

This technique would iterate to a fairly low normalized mean square error and then on the next iteration fluctuate to a high (above one in some cases) normalized mean square error. Table 4 lists representative convergence characteristics of this technique for the cases simulated. In many cases simulated the lowest mean square error achieved was on the first iteration. The poor convergence characteristics of this technique make it unacceptable.

The second feedback technique simulated differs from the first technique in that the guessed aperture wavefront is always zero outside the aperture. Simulations of this technique indicate that it has good convergence properties. Table 5 lists simulation results for a feedback function where the imaginary component of the output aperture field ($\hat{f}_{a2}(x_a)$) is used (equation (57), FB_3). This feedback technique is able to approximate the phase of aperture wavefronts that have Linear, Sine, Cosine and Constant (trivial) aperture aberations, with a normalized mean square error that is less than 6.1E-2 and requiring about 10 iterations. This technique could not retrieve the random phase aberations well; for the case simulated (Table 5, case 5) the best normalized mean square error achieved is 8.5E-1 on the fifth iteration (stopped converging on this iteration). This technique requires 0.015cp execution seconds per iteration.

Interesting characteristics of the Gerchberg-Saxton Algorithm with the second feedback technique are: that

#ITT	Aperture Phase	
	Linear (NMSE)	Sine (NMSE)
1	5.4E-2	9.6E-1
2	2.0E-1	1.4E+0
3	1.7E-1	3.4E-1
4	4.1E-2	2.1E-1
5	6.5E-2	2.4E-1
6	3.5E-2	2.2E-1
7	7.3E-2	1.5E-1
8	3.6E-2	2.1E-1
9	5.8E-2	1.9E-1
10	7.6E-2	1.9E-1
50	7.3E-2	1.8E-1
100	7.4E-2	1.8E-1
500	8.0E-2	1.6E-1

Init guess of Aperture Field = $1 + j \text{random1}(x_a)$

Feedback = $B(\hat{f}_{a2}(x_a)) = 1 (FB_2)$

Table 4. Representative Convergence Characteristics of the Gerchberg-Saxton Algorithm with the First Feedback Technique

Aperture Phase	NMSE	#ITT	Init guess of Aperture Field
1. Const	3.8E-29	1	$1+j0$
	2.8E-1	1	$1+j\text{random1}(x_a)/10$
	5.5E-3	5	$1+j\text{random1}(x_a)/10$
	2.4E-4	20	$1+j\text{random1}(x_a)/10$
	1.4E-4	30	$1+j\text{random1}(x_a)/10$
2. Linear	1.7E-2	1	$1+j0$
	7.3E-3	3	$1+j0$
	1.2E-3	10	$1+j0$
	4.5E-4	20	$1+j0$
3. Sine	7.0E-2	1	$1+j0$
	1.0E-4	2	$1+j0$
	1.0E+0	1	$1+j\text{random1}(x_a)/10$
	1.4E-1	10	$1+j\text{random1}(x_a)/10$
4. Cosine	1.0E+0	1	$1+j0$
	9.6E-2	1	$1+j\text{random1}(x_a)/10$
	6.1E-2	2	$1+j\text{random1}(x_a)/10$
5. $\text{Random1}(x_a)/10$	8.8E-1	1	$1+j\text{random1}(x_a)/10$
	8.5E-1	5	$1+j\text{random1}(x_a)/10$
	8.5E-1	10	$1+j\text{random1}(x_a)/10$

$$\text{Feedback} = B(\hat{f}_{a2}(x_a)) = 1(FB_3)$$

Table 5. Simulation Results - Gerchberg-Saxton Algorithm with the Second Feedback Technique

odd aperture aberations (Table 5, case 4) converge to its
unique solution and retrieved the phase of the aperture
field without bias errors, unlike the Gerchberg-Saxton
Algorithm without feedback.

This chapter defines the aperture wavefronts used
in the simulations, the measure of performance, and presents
the data and performance analysis of the phase retrieval
techniques simulated. The Phase Numeric 1 Technique
yielded unacceptable performance. The Phase Numeric
2 Technique is able to approximate linear phase aberations
(tilt) in the aperture field, but could not approximate
more complicated aberations. This technique required
approximately 250cp execution seconds to reconstruct a
linear aberation. The Gerchberg-Saxton Algorithm yielded
the best performance of the techniques investigated
converging to a solution in most simulation runs within
0.075cp execution seconds.

V Conclusion

Retrieval of the phase of the aperture field from
intensity measurements in the focal plane of an imaging
sensor is possible. The aperture phase although not
explicitly present, is contained in the intensity dist-
ribution in the focal plane of an imaging sensor. Phase
retrieval techniques studied in this project were simulated
for an aperture field which is a function of one spatial
variation (one-dimensional fields). Three techniques
simulated are able to retrieve the phase of an aperture
field with various success; these techniques are: the
Phase Numeric 2 Technique, the Gerchberg-Saxton Algorithm
without feedback, and the Gerchberg-Saxton Algorithm with
the second feedback technique.

The Phase Numeric 2 Technique is a brute force method
which optimizes the Fourier series coefficients as a means
to infer the aperture phase. This technique is able to
retrieve Linear phase aberations, with a normalized mean
square error of 2.2E-1 (requiring 250cp execution seconds
to converge to a solution), but can not retrieve more
complicated aperture phase aberations.

The Gerchberg-Saxton Algorithm (without feedback) has
the best performance of the techniques simulated in this
research project. The Gerchberg-Saxton Algorithm converges

to a solution with a normalized mean square error less than 1.6E-1 (in less than 0.15cp execution seconds) for all aperture phase aberations simulated except for aperture phase aberations with large random fluctuations. The Gerchberg-Saxton Algorithm with the second feedback method is able to retrieve the aperture phase of the wavefronts simulated with a normalized mean square error less than 6.1E-2 (in less than 0.15cp execution seconds), except for aperture phase aberations with random fluctuations.

Suggestions for Further Study

An area of recommended research is to investigate the technique developed in this study for the computation of the magnitude of the Fourier series coefficients using the autocorrelation function of the aperture plane. This information from the focal plane intensity measurements has the potential of improving the performance of the Phase Numeric 2 Technique.

Another issue worthy of investigation is to determine how the Gerchberg-Saxton Algorithm Techniques and the Phase Numeric 2 Technique perform with an aperture field that is a function of two spatial variations (two-dimensional fields). Additional analysis should then be preformed to determine the convergence sentivities of these approaches in the presence of noise and non-exact intensity measurements in the focal plane of the imaging sensor.

Bibliography

1.   Fried, D.L.,   "Propagation of a Spherical Wave in a
      Turbulent Medium," J. Opt. Soc. Am., Vol 57, No 2, 1967.

2.   Hardy, J.W.,   "Active Optics: A New Technology for the
      Control of Light," Proceedings of the IEEE, Vol 66, No 2,
      1978.

3.   Francon, M., Optical Interferometry, Academic Press,
      New York, 1966.

4.   Robinson, S.R.,   "On the Problem of Phase From Intensity
      Measurements," J. Opt. Soc. Am., Vol 68, No1, 1978.

5.   Gonsalves, R.A.,   "Phase Retrieval From Modulus Data,"
      J. Opt. Soc. Am., Vol 66, No 9, 1976.

6.   Southwell, W.H.,   "Wavefront Analyser Using a Maximum
      Liklihood Algorithm," J. Opt. Soc. Am., Vol 67, No 3,
      1977

7.   Gerchberg, R.W. and W.O. Saxton,   "A Practical Algorithm
      for the Determination of Phase From Image and Diffraction
      Plane Pictures", Optik 35, 1972.

8.   Fienup, J. r.,   "Reconstruction of an Object From the
      Modulus of its Fourier Transform," Opt. Soc. Am. Letters,
      Vol 3, 1978.

9.   Goodman, J., Introduction to Fourier Optics, McGraw-Hill,
      San Francisco, 1968.

10.   Couraht, R. and D. Hilbert, Methods of Mathematical
      Physics, Interscience Publishers, New York, 1953.

11.   Papoulis, A., Probability, Random Variables, and
      Stochastic Processes, McGraw-Hill, New York, 1965.

12.   Davenport, W.B. Jr., Probability and Random Processes,
      McGraw-Hill, New York, 1970.

13.   International Mathematical Statistical Libraries (IMSL),
      IMSL Library Reference Manual, Houston, 1975.

14.   Fletcher, R.,   "Fortran Subroutines for Minimization by
      Quasi-Newton Methods," Report R7125 AERE, Harwell, England.

15. Born, M. and E. Wolf, _Principales of Optics_, Pergamon Press, New York, 1975.

16. Gagliardi, R.M. and S. Karp, _Optical Communications_, Wiley-Interscience, New York, 1976.

17. Gaskill, J.D., _Linear Systems, Fourier Transforms, and Optics_, Wiley and Sons, New York, 1978.

18. Hogge, C.B. and R.R. Butts, "Frequency Spectra for the Geometric Representation of Wavefront Distortions Due to Atmospheric Turbulence," _IEEE Transactions of Antennas and Propagation_, _Vol AP-24_, No 2, 1976.

19. Jacoly, S.L.S. etal, _Iterative Methods for Nonlinear Optimization Problems_, Prentice-Hall, New Jersey, 1972.

20. Oppenheim, A.V. and R.W. Schafer, _Digital Signal Processing_, Prentice-Hall, New Jersey, 1974.

21. Papoulis, A., _The Fourier Integral and its Applications_, McGraw-Hill, New York, 1962.

Vita

Charles V. Scull was born on 21 September 1951 in New York City, N.Y.. He is the son of Charles Y. Scull and Catherine A. (Tesoriero) Scull. He graduated from T.A. Edison Technical High School in June of 1969, and attended York College of the City University of New York from August 1969 to January 1971. He enlisted in the United States Air Force (USAF) on 5 February 1971 and served as a Precision Measurement Laboratory Technician. On 15 January 1975 he graduated from the University of Illinois, Champaign-Urbana and was awarded the Bachelor of Science degree with High Honors. Upon graduation from Officer Training School, on 24 March 1975, he recieved a commission as a second lieutenant in the USAF. He worked as a Development Engineer in the Air Force Avionics Laboratory, Wright-Patterson AFB, Oh. until assigned to the Air Force Institute of Technology, School of Engineering, in June 1978 as a resident graduate student.

Permanent address: 261-15 Langston Avenue
                    Glen Oaks, New York 11004

REPORT DOCUMENTATION PAGE		READ INSTRUCTIONS BEFORE COMPLETING FORM
1. REPORT NUMBER AFIT/GEO/EE/79-4	2. GOVT ACCESSION NO.	3. RECIPIENT'S CATALOG NUMBER
4. TITLE (and Subtitle) PHASE RETRIEVAL USING AN IMAGING SENSOR		5. TYPE OF REPORT & PERIOD COVERED
		6. PERFORMING ORG. REPORT NUMBER
7. AUTHOR(s) Charles V. Scull Capt., USAF		8. CONTRACT OR GRANT NUMBER(s)
9. PERFORMING ORGANIZATION NAME AND ADDRESS Air Force Institute of Technology Wright-Patterson AFB, Oh 45324		10. PROGRAM ELEMENT, PROJECT, TASK AREA & WORK UNIT NUMBERS
11. CONTROLLING OFFICE NAME AND ADDRESS Air Force Weapons Laboratory (ALO) Air Force Systems Command Kirtland AFB, NM 87115		12. REPORT DATE
		13. NUMBER OF PAGES 64
14. MONITORING AGENCY NAME & ADDRESS(if different from Controlling Office)		15. SECURITY CLASS. (of this report) UNCLASSIFIED
		15a. DECLASSIFICATION/DOWNGRADING SCHEDULE

16. DISTRIBUTION STATEMENT (of this Report)

Approved for public release;   distribution unlimited

17. DISTRIBUTION STATEMENT (of the abstract entered in Block 20, if different from Report)

18. SUPPLEMENTARY NOTES
Approved for public release;   IAW AFR 190-17

JOSEPH P. HIPPS, Major, USAF
Director of Information

19. KEY WORDS (Continue on reverse side if necessary and identify by block number)

Phase retrieval	Signal processing
Imaging sensor	Intensity
Spatial Fourier transform	
Fourier optics	
Aperture wavefront	

20. ABSTRACT (Continue on reverse side if necessary and identify by block number)
Work was completed which investigates the retrieval of the spatial phase of the aperture wavefront from sampled intensity data in the focal plane of an imaging sensor, where phase is not explicity present. Techniques investigated are signal processing methods that use the Fourier transform properties of a lens, analytics and numerics to retrieve the spatial phase. Simulations of these methods are compared yielding the Gerchberg-Saxton Algorithm as the most promising technique to approximate the spatial phase.

DD , FORM 1473 JAN 73   EDITION OF 1 NOV 68 IS OBSOLETE